Lasing from Excitons in Quantum Wires

W. Wegscheider, L. N. Pfeiffer, M. M. Dignam, A. Pinczuk, K. W. West, S. L. McCall, and R. Hull
AT&T Bell Laboratories, Murray Hill, New Jersey 07974
(Received 20 September 1993)

Stimulated optical emission from the lowest exciton state in atomically smooth semiconductor quantum wires is observed for the first time. The wires are formed by the T intersection of two 7 nm GaAs quantum wells. The optical emission wavelength is nearly independent of pump levels. This absence of band-gap renormalization in the laser emission indicates a marked increase in the stability of the exciton in one dimension.

PACS numbers: 78.45.+h, 73.20.Dx, 78.55.Cr

The superior performance of quantum well (QW) semiconductor lasers over heterostructure lasers has directed considerable attention towards lower-dimensionality quantum wire (QWR) and quantum box structures. Carrier confinement to one or even zero dimensions is expected to give rise to sharp peaks in the density of states. This should lead to a variety of interesting optical properties such as increased exciton binding [1,2], enhanced optical nonlinearities [3], narrower gain spectra, and higher differential gain [4]. These striking physical phenomena are of importance for novel optoelectronic devices. Quantum wire geometries have been proposed as a route to lower threshold lasers having reduced threshold temperature sensitivity and increased modulation bandwidth [4–6]. However, the fabrication of QWR structures with precisely controlled dimensions is a very challenging task. Growth on patterned substrates [7] has been used to fabricate QWRs exhibiting optical signatures of carrier confinement to one dimension. In that work, stimulated emission from QWRs was first demonstrated. However, the relatively large size (80–100 by 10 nm) of the structures results in the occupation of many one-dimensional (1D) subbands, and due to band-filling effects only the higher-order transitions were observed.

The existence of QWR states was recently also demonstrated at the T intersection of two GaAs QWs [8]. The T concept originally proposed by Chang *et al.* [9] was realized by the cleaved edge overgrowth (CEO) method, a molecular beam epitaxy (MBE) technique that uses high-quality regrowth on the cleaved edge of a multilayer sample [10]. The method is capable of producing nearly perfect structures with atomic control in two dimensions. The quantum mechanical bound state of an electron at two intersecting QWs is illustrated in Fig. 1. Near the T intersection confinement is somewhat relaxed leading to a smaller kinetic contribution to the total energy. A carrier in such a bound state is free to move along the line defined by the intersecting planes of the two QWs.

This Letter reports the first observation of stimulated optical emission using exciton recombination in QWRs formed at intersecting GaAs QWs. Exciton emission in the 1D quantum limit, i.e., from the ground state exciton, is apparent in these structures at low optical pump power densities of 600 W/cm^2, where the adjacent QWs show no stimulated emission. Equally striking is the near constancy of the photon emission energy of the QWRs under large changes of pump power, ranging over 2 orders of magnitude to 3 kW/cm^2. The absence of redshifts due to band-gap renormalization, that are characteristic of an electron-hole plasma, shows that the optical recombination is excitonic for all pump intensities in the present experiments. On the basis of these results we conclude that the observed laser emission is due to excitonic gain [11]. Enhancement of the exciton binding energy, due to confinement of the electron and hole to the QWRs, is consistent with these results. Excitonic laser emission has not been previously observed in lasers fabricated from III-V semiconductors. It thus appears that in wires at intersecting QWs the 1D exciton gas phase is highly stable against formation of an electron-hole plasma.

A schematic cross-sectional view of the QWR laser structure is shown in Fig. 2. The CEO growth method consists of several steps [10]. The first MBE growth on a (001) GaAs semi-insulating substrate consists of a 1 μm $Al_{0.5}Ga_{0.5}As$ cladding layer followed by a 22-period $GaAs/Al_{0.35}Ga_{0.65}As$ multiple quantum well (MQW) structure with well and barrier thicknesses of 7 and 38 nm, followed by a 3 μm $Al_{0.5}Ga_{0.5}As$ cladding layer. The sample is then removed from the MBE machine, mechanically thinned from the backside and reinserted into the

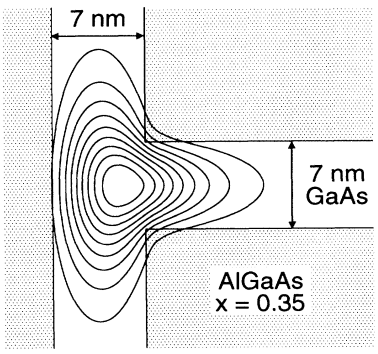

FIG. 1. T-shaped intersection of two quantum wells in cross section. The contours are lines of constant probability ($|\psi|^2 = 0.1, 0.2, \ldots, 0.9$) for electrons confined in the quantum wire.

0031-9007/93/71(24)/4071(4)$06.00

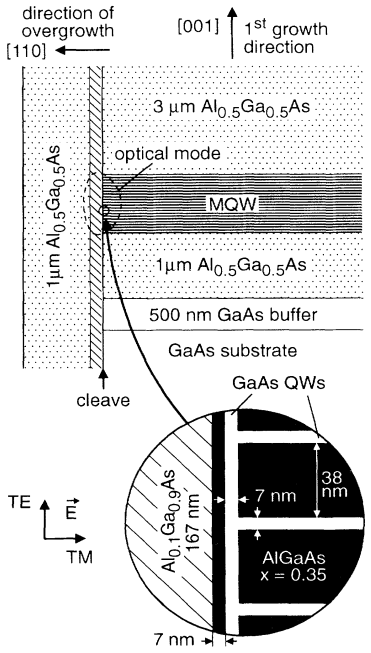

FIG. 2. Schematic cross section of the quantum wire laser structure. The MQW layer consists of 22 GaAs quantum wells separated by $Al_{0.35}Ga_{0.65}As$ barriers as illustrated in the magnified part of the quantum wire region. The mirrors were cleaved perpendicular to the quantum wire axis defined by the line of intersection. The dashed line represents a contour plot of the optical mode at 10% of the maximum intensity.

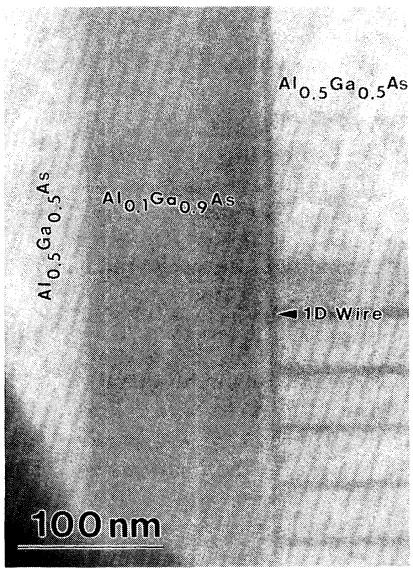

FIG. 3. Cross-sectional bright-field transmission electron micrograph of the T-shaped quantum wire structure taken in the [$\bar{1}$10] zone axis, i.e., with the electron beam aligned along the quantum wire axis. Dark areas correspond to GaAs or GaAs rich regions. The location of one T-shaped quantum well intersection is marked by an arrow.

growth chamber. An *in situ* cleave is performed and within seconds the second MBE overgrowth is started on the fresh (110) surface exposed by the cleave. The post-cleave growth sequence consists of a 7 nm wide GaAs QW followed by a 7 nm wide $Al_{0.35}Ga_{0.65}As$ barrier, a 167 nm wide $Al_{0.1}Ga_{0.9}As$ layer, and a 1 μm wide $Al_{0.5}Ga_{0.5}As$ cladding layer. As can be seen in the cross-sectional transmission electron micrograph of the QWR laser structure depicted in Fig. 3, T-shaped QW intersections form along the cleavage plane. The high degree of structural perfection of the QWRs attainable by the CEO method is manifested by the planarity and abruptness of the interfaces along both growth directions. Note also the absence of any defects originating from the (110) cleave which served as the starting plane for the second MBE growth step. The cladding layers serve as a T-shaped dielectric waveguide confining an optical mode in the vicinity of the QWR array (see Fig. 2), according to waveguide calculations within an effective refractive index approximation.

After the second MBE growth the samples were again cleaved so as to form optical cavities of length $L = 600$ μm bounded by mirrors perpendicular to the axis of the QWRs. The cleave mirrors were left uncoated so that each mirror had a reflectivity of about 0.3. Continuous wave optical excitation of samples immersed in superfluid He was performed using the output of a dye laser tuned to $\lambda = 775$ nm. At this wavelength significant light absorption occurs only in the GaAs layers. The pump laser beam was incident on the (001) growth surface and was focused using two cylindrical lenses and a multielement 0.2 numerical aperture lens to a stripe of about 700 μm in length and 5 μm in width oriented parallel to the QWRs. However, because the QWR volume is so small, light absorption takes place mainly in the QWs. Light transmitted through one of the cleavage mirrors was dispersed in a 0.85 m double monochromator and detected with a charge-coupled-device camera.

Figure 4 compares polarized emission spectra below and above threshold for stimulated emission in the QWRs, observed from the cleaved end of a laser sample. At low excitation power (lower panel of Fig. 4) the two major features are due to excitonic emission from the QWRs and QWs [8]. The QWR luminescence is red-shifted by about 15 meV with respect to the QW signal at about 1.58 eV. The doublet structure in the QW emission is believed to originate from slightly different confinement energies for the MQWs grown along the [001] direction and the [110] oriented QW formed during overgrowth. Even at this low excitation power (0.25 mW), the QWR spectra show closely spaced Fabry-Pérot oscillations corresponding to different longitudinal modes within the optical waveguide cavity. The unusually strong contrast in the Fabry-Pérot oscillations, which develop on the low energy side, indicates a high degree of transparency in the

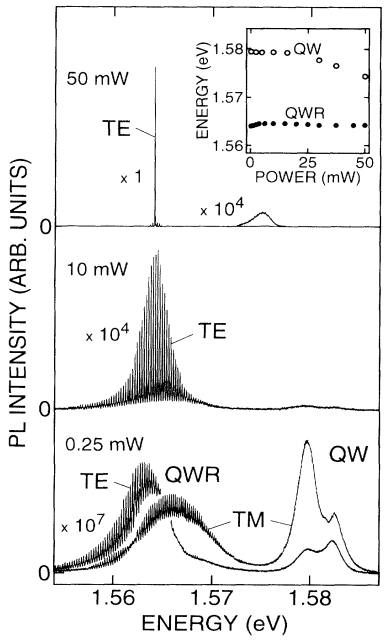

FIG. 4. TE-polarized photoluminescence spectra recorded at different excitation below, just above, and about 5 times above threshold for stimulated emission in the quantum wires. A TM-polarized spectrum, only seen at the lowest pump power, is also shown. The direction of the **E** vector for the two polarization directions is given in Fig. 2. Inset: Power dependency of the quantum well (QW) and quantum wire (QWR) photoluminescence energies.

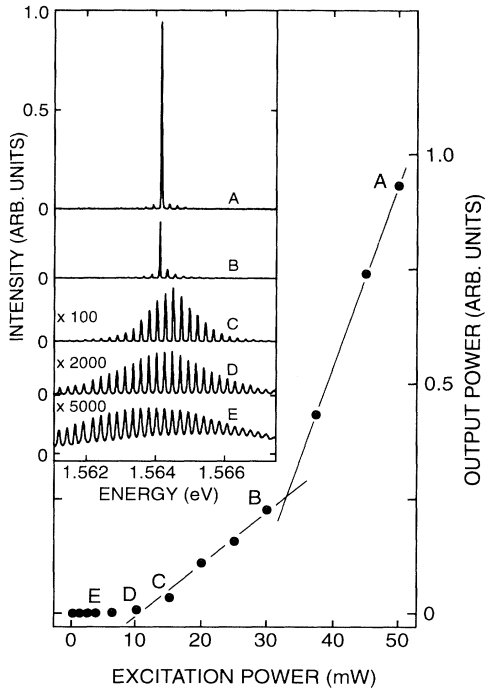

FIG. 5. Output vs excitation power characteristic for a cavity length of 600 μm and uncoated mirrors. Inset: Evolution of the TE-polarized emission spectra with increasing pump power.

waveguide within this spectral region. This is expected because of the small fraction Γ of the optical intensity distribution, of about 3×10^{-3}, that overlaps the QWRs. For comparison, the corresponding value for the QWs is $\Gamma \sim 0.15$.

Stimulated emission spectra of the QWR laser sample are displayed in the upper portion of Fig. 4 and in the inset of Fig. 5. The QW peak intensity increases linearly with excitation power below 10 mW, and increases sublinearly above. In contrast, striking superlinear behavior is seen for the QWR emission. The QW luminescence line redshifts with increasing power by as much as 5 meV. This shift is the experimental signature of band-gap renormalization caused by photoexcitation of an electron-hole plasma in the QW. The QWR emission again in contrast shows no redshift at any pump power (see inset of Fig. 4), implying that an electron-hole plasma never forms in the QWRs. From this argument we conclude that exciton and not free carrier recombination is the gain mechanism in our QWR laser.

In order to further understand this behavior we estimate the carrier densities present in the QWRs and QWs. The 50 mW excitation corresponds to a power density of $\sim$3 kW/cm^2. Assuming an absorption length of 0.5 μm in GaAs and a surface reflectivity R of 0.3, this corresponds to a rate of $\sim10^{20}$ e-h pairs/cm^2 s generated in the individual QWs. With a recombination time of 1 ns in the QWs [12] we expect a sheet carrier density of $\sim10^{11}$ e-h pairs/cm^2. The shrinkage of the free-particle band gap due to band-gap renormalization for this carrier density is about 15 meV [13]. This value exceeds the QW exciton binding energy by about 5 meV, consistent with the notion that QW luminescence is due to exciton recombination with excitation less than 25 mW, and band to band above. Despite the much smaller volume of the QWRs their luminescence intensity equals or exceeds that of the QWs at all powers. This can be attributed to two effects: (i) Carriers, most of which are generated in the QWs drain into the QWR region. Assuming comparable lifetimes in the QWs and QWRs, carriers diffusing from 1 μm into the QWRs would lead to $\sim10^6$/cm carrier density at 5 mW pump power, which turns out to be approximately the inverse of a 1D exciton diameter. (ii) In 1D the oscillator strength is predicted to be strongly concentrated on the lowest exciton state [14]. As seen in Fig. 4, observation of excitonic emission in the QWRs even at the highest excitation levels, at which the 2D excitons in the QWs are ionized, clearly demonstrates the enhanced stability of the 1D exciton gas phase. This is in marked contrast to GaAs heterostructure lasers, which operate in the regime of a degenerate electron-hole plasma. To the best of our knowledge, this represents the first GaAs laser structure whose gain is not due to free carrier recombination. Variation of the QWR emission with excitation

power shown in Fig. 5 is characterized by a crossover between points labeled B and C from a multimode spectrum to single line laser operation. As can be seen from the output characteristic of the laser, this transition is accompanied by an increase in the differential quantum efficiency. Luminescence from within a Fabry-Pérot interferometer shows intensity oscillations with a contrast ratio $[1 + R\exp(-\alpha L)]^2/[1 - R\exp(-\alpha L)]^2$, where α is the frequency dependent absorptivity. With $\alpha = 0$ the contrast ratio is about 3.45. Referring to the spectrum labeled D in Fig. 5, the contrast is seen to greatly exceed this $\alpha = 0$ value, so that the absorption constant must be negative; i.e., there is considerable gain. The slope change in Fig. 5 at point D is not where the lasing instability occurs, but is associated with strong amplification of intracavity light.

The 1D character of the QWR emission is also reflected in the polarization behavior below threshold. The TE- and TM-polarized luminescence are of nearly equal intensities, although of different width and separated by about 3 meV. The fundamental energy transition in the QWRs which is strongly polarized along the TE direction gives rise to a 4 meV wide peak at 1.564 eV. The large width of the TM-polarized luminescence of about 8 meV strongly suggests the presence of several transitions in this spectral region, which we believe involve closely spaced hole states in our QWRs. On a qualitative basis we can interpret the occurrence of luminescence peaks of equal intensities in both polarizations as a property of the reduced dimensionality since the emission from a QWR with symmetrical cross section would be isotropic neglecting the anisotropy of the valence band.

In order to estimate the binding energy of the 1D excitons in our structure we have carried out a calculation of the electron (see Fig. 1) and hole wave functions and confinement energies for the T-shaped confining potential in the absence of the e-h Coulomb interaction using a two-dimensional transfer matrix technique [15,16]. For the electron-heavy hole transition in the QWRs we obtain a redshift of 10 meV from the corresponding QW transition. The experimentally observed shift is about 17 meV. Since both the QWR and the QW transition at this low excitation level ($\sim$15 W/cm^2) are undoubtly of excitonic nature, the energy difference of about 7 meV directly reflects the enhancement of the exciton binding energy due to the reduced dimensionality. Taking a 2D exciton binding energy of 10–11 meV [17,18] for the 7 nm wide QWs into account, we obtain a 1D enhancement of about 50% to about 17 meV for the QWRs. This considerably exceeds the largest previously reported 1D enhancement of 15% observed in 70 by 14 nm lithographically defined structures [19].

In summary, laser emission from 1D excitons in QWRs is observed for the first time. The continuous evolution of the emission from low power exciton luminescence to an intense single mode lasing line with no energy shift demonstrates excitonic gain even at the highest powers and suggests interesting new behavior for excitons in one dimension.

It is a pleasure to acknowledge helpful discussions with H. L. Stormer, N. K. Dutta, M. S. Hybertsen, A. F. J. Levi, and R. E. Slusher, focused ion beam sample preparation by F. Stevie, and technical assistance from B. S. Dennis and D. Bahnck.

[1] M. H. Degani and O. Hipolito, Phys. Rev. B **35**, 9345 (1987).
[2] L. Bányai, I. Galbraith, C. Ell, and H. Haug, Phys. Rev. B **36**, 6099 (1987).
[3] S. Schmitt-Rink, D. A. B. Miller, and D. S. Chemla, Phys. Rev. B **35**, 8113 (1987).
[4] Y. Arakawa and A. Yariv, IEEE J. Quantum Electron. **22**, 1887 (1986).
[5] Y. Arakawa and H. Sakaki, Appl. Phys. Lett. **40**, 939 (1982).
[6] M. Asada, Y. Miyamoto, and Y. Suematso, IEEE J. Quantum Electron. **22**, 1915 (1986).
[7] E. Kapon, D. M. Hwang, and R. Bhat, Phys. Rev. Lett. **63**, 430 (1989).
[8] A. R. Goñi, L. N. Pfeiffer, K. W. West, A. Pinczuk, H. U. Baranger, and H. L. Stormer, Appl. Phys. Lett. **61**, 1956 (1992).
[9] Y. C. Chang, L. L. Chang, and L. Esaki, Appl. Phys. Lett. **47**, 1324 (1985).
[10] L. Pfeiffer, K. W. West, H. L. Störmer, J. P. Eisenstein, K. W. Baldwin, D. Gershoni, and J. Spector, Appl. Phys. Lett. **56**, 1697 (1990).
[11] J. Ding, H. Jeon, T. Ishihara, M. Hagerott, and A. V. Nurmikko, Phys. Rev. Lett. **69**, 1707 (1992).
[12] J. Feldmann, G. Peter, E. O. Göbel, P. Dawson, K. Moore, C. Foxon, and R. J. Elliot, Phys. Rev. Lett. **59**, 2337 (1987).
[13] S. Schmitt-Rink, D. S. Chemla, and D. A. B. Miller, Adv. Phys. **38**, 89 (1989).
[14] T. Ogawa and T. Takagahara, Phys. Rev. B **43**, 14325 (1991); **44**, 8138 (1991).
[15] M. M. Dignam (unpublished).
[16] We have employed a one-band model for the hole, with masses determined via the diagonal term in the Luttinger Hamiltonian with the angular momentum quantization axis parallel to the [110] overgrowth direction.
[17] R. L. Greene, K. K. Bajaj, and D. E. Phelps, Phys. Rev. B **29**, 1807 (1984).
[18] L. C. Andreani and A. Pasquarello, Phys. Rev. B **42**, 8928 (1990).
[19] M. Kohl, D. Heitmann, P. Grambow, and K. Ploog, Phys. Rev. Lett. **63**, 2124 (1989).

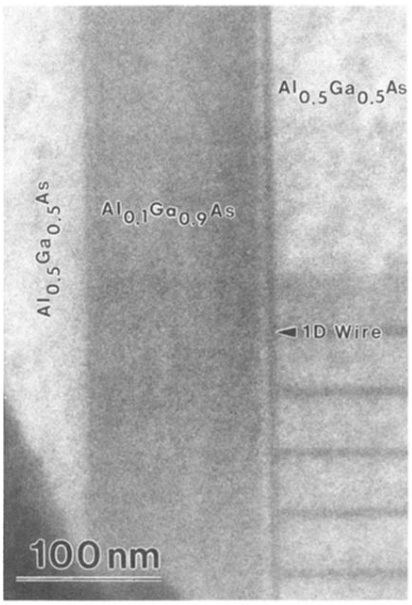

FIG. 3. Cross-sectional bright-field transmission electron micrograph of the T-shaped quantum wire structure taken in the [$\bar{1}$10] zone axis, i.e., with the electron beam aligned along the quantum wire axis. Dark areas correspond to GaAs or GaAs rich regions. The location of one T-shaped quantum well intersection is marked by an arrow.